

Reduced Choroidal Neovascular Membrane Formation in Cyclooxygenase-2 Null Mice

Kasra A. Rezaei,¹ Hassanain S. Toma,¹ Jiyang Cai,¹ John S. Penn,^{1,2,3} Paul Sternberg,¹ and Stephen J. Kim¹

PURPOSE. To assess the degree of laser-induced choroidal neovascular membrane formation in wild-type (WT) and COX-2 null mice and to measure vascular endothelial growth factor (VEGF), interleukin (IL)-1 β , and tumor necrosis factor (TNF)- α levels in the retina and choroid.

METHODS. Four laser burns were placed in each eye of WT and COX-2 null mice to induce choroidal neovascularization. Fluorescein angiography (FA) was performed at 14 days, and retinal pigment epithelium-choroid-sclera (choroidal) flat mounts were prepared. The retina and choroid were isolated from WT and COX-2 null mice at 24, 72, and 168 hours after laser photocoagulation and from unlasered eyes and were tested for VEGF, IL-1 β , and TNF- α .

RESULTS. COX-2 null mice demonstrated 58% ($P = 0.001$) and 48% ($P = 0.001$) reductions in CNV formation on FA and choroidal flat mounts, respectively, compared with WT mice. For unlasered mice, mean VEGF concentrations in the retina and choroid were 1.2 ± 0.42 pg/mg protein for WT but only 0.42 ± 0.2 pg/mg protein for COX-2 null mice ($P < 0.05$). After laser photocoagulation, WT mice showed significantly greater VEGF and IL-1 β expression in the retina and choroid by 168 hours ($P < 0.05$) and 72 hours ($P < 0.05$), respectively, compared with COX-2 null mice.

CONCLUSIONS. COX-2 null mice exhibited significantly less choroidal neovascular membrane formation associated with reduced expression of VEGF. The results of this study suggest that COX-2 modulates VEGF expression in CNV and implicates a potential therapeutic role for nonsteroidal anti-inflammatory drugs. (*Invest Ophthalmol Vis Sci.* 2011;52:701-707) DOI: 10.1167/iovs.10-6319

Choroidal neovascularization (CNV) is a leading cause of severe vision loss in patients with age-related macular degeneration (AMD) and contributes to substantial vision loss in posterior uveitis,¹ pathologic myopia,² and ocular histoplasmosis.³ Although the pathogenesis of CNV is multifactorial, a growing body of scientific evidence suggests that cyclooxygenase plays a contributory role.⁴⁻⁶

From the ¹Department of Ophthalmology and Visual Sciences, Vanderbilt University Medical Center, Nashville, Tennessee; and the Departments of ²Pharmacology and ³Cell and Developmental Biology, Vanderbilt University School of Medicine, Nashville, Tennessee.

Supported in part by National Institutes of Health Grants EY07533 (JSP) and EY07892 (PS), National Eye Institute Core Grant EY08126, and an unrestricted grant from Research to Prevent Blindness.

Submitted for publication August 1, 2010; revised August 22, 2010; accepted September 3, 2010.

Disclosure: **K.A. Rezaei**, None; **H.S. Toma**, None; **J. Cai**, None; **J.S. Penn**, None; **P. Sternberg**, None; **S.J. Kim**, None

Corresponding author: Stephen J. Kim, Department of Ophthalmology and Visual Sciences, Vanderbilt University Medical Center, 2311 Pierce Avenue, Nashville, TN 37232; skim30@gmail.com.

Cyclooxygenase (COX) is an important enzyme in the inflammatory process and catalyzes the biosynthesis of prostaglandins from membrane-bound arachidonic acid. Two isoforms of COX, COX-1 and COX-2, are firmly established. COX-1 is constitutively expressed in almost all tissues and is responsible for normal housekeeping functions. In contrast, COX-2 expression is induced by a wide variety of pathologic and physiologic stimuli. In the human retina, COX-2 has been shown to be the predominant isoform in human retinal pigment epithelium (RPE) and is significantly upregulated by pro-inflammatory cytokines.⁷

Prostaglandins have wide-ranging effects within the eye, including vasodilation, disruption of the blood-ocular barrier, and facilitation of leukocyte migration. Accumulating evidence suggests that prostaglandins may also promote CNV.⁸ In support of this, COX-2 can be detected in human choroidal neovascular membranes,⁹ and pharmacologic inhibition of COX-2 suppresses choroidal neovascular growth in a variety of experimental systems.^{4,5,10,11}

To more firmly establish the role of COX-2 in choroidal neovascularization, we assessed the formation of CNV in wild-type (WT) and COX-2 null mice using the well-established laser-induced model. Furthermore, we investigated the relationship between COX-2 and vascular endothelial growth factor (VEGF) and several other inflammatory cytokines in CNV.

METHODS

All procedures were performed with strict adherence to guidelines for animal use and experimentation set forth by the Vanderbilt University Animal Care and Use Committee and the ARVO Statement for the Use of Animals in Ophthalmic and Vision Research and were approved.

Animals

Wild-type (WT) C57/129 mice and COX-2 null mice on the same background (breeders were a generous gift from Sudhansu Dey, Cincinnati Children's Hospital Medical Center) and at the same age (6 weeks) were used in all experiments. Animals were maintained in a controlled environment with a 12-hour on/12-hour off light cycle. Food was available ad libitum. For all procedures, animals were anesthetized by intramuscular injection of ketamine hydrochloride (80 mg/kg) and xylazine hydrochloride (12 mg/kg). Pupils were dilated with phenylephrine (2.5%) and atropine sulfate (1%). Proparacaine (0.5%) was applied for corneal anesthesia.

Laser Photocoagulation

Laser photocoagulation was performed using a method similar to that described by Edelman and Castro.¹² WT and COX-2 null mice were positioned before a slit lamp (Carl Zeiss Meditec, Jena, Germany) laser delivery system, and the fundus was visualized using a microscope slide coverslip with 2.5% hydroxypropyl methylcellulose solution as an optical coupling agent. An argon green laser (Coherent, Santa Clara, CA) was used for photocoagulation with settings of 532-nm wave-

length, 260-mW power, 0.07-second duration, and 50- μ m spot size most reliably producing acute vapor bubbles indicative of the rupture of Bruch's membrane. In each eye, four focal laser spots were applied concentrically approximately two optic disc areas from the optic nerve center, avoiding major blood vessels. No eyes were excluded because of vitreous hemorrhage or cataract.

Assessment of CNV Formation

To quantify choroidal neovascular growth, six WT and six COX-2 null mice underwent fluorescein angiography (FA) on day 14 after laser treatment. For FA evaluations, 0.1 mL of 10% sodium fluorescein was administered intraperitoneally, and photographs of the right and left eye were taken. Angiograms consistent with early-mid phase (approximately 4–6 minutes after injection of fluorescein) were used for all comparative analyses.

After FA imaging, animals were euthanized by cervical dislocation, and eyes were enucleated and stored in 10% formalin for 2 hours. RPE-choroid-sclera (choroidal) flat mounts were prepared as previously described.¹² The cornea and lens were removed. After dissecting the retina from the eyecup and discarding it, radial cuts were made in all four quadrants to flatten the remaining tissue. The flattened RPE-choroid-sclera tissue was then mounted in medium (Gel Mount; Biomedica, Victoria, Australia). Endothelial cells were identified using FITC-conjugated *Bandeiraea simplicifolia* isolectin B4, (Sigma-Aldrich, Inc., St. Louis, MO), and the elastin of the surrounding extracellular matrix was stained using goat anti-elastin antibody conjugated to Cy3 (Santa Cruz Biotechnology, Inc., Santa Cruz, CA). Choroidal flat mounts were visualized using the 10 \times objective of an epifluorescent compound microscope fitted with the appropriate excitation and emission filters (Provis AX-70; Olympus, Tokyo, Japan). Images of the neovascular lesions were captured using a digital camera attached to the Provis system (DP71; Olympus) coupled to a computer with image capture software (DP Controller; Olympus).

Quantitative Analysis of CNV

CNV staining and leakage on FA and vascular budding on choroidal flat mounts were calculated by measuring the pixel area within the circumference of each rupture site using image editing software (Photoshop CS3; Adobe Systems Inc., San Jose, CA), as previously described.¹³ CNV lesions on FA were measured by a trained, masked investigator, using the Quick Selection Tool in the software (Photoshop CS3; Adobe) to measure the pixel area contained within the best-fitting polygon. Laser rupture sites that had subretinal bleeding at the time of lasering were excluded from analysis and represented <10% of total rupture sites in each group. On choroidal mounts, the pixel area of vascular budding was traced by a trained, masked investigator using the Lasso selection tool in the software (Photoshop CS3; Adobe). The cross-sectional area of each CNV lesion was quantified as the area contained within the best-fitting polygon.

Expression of VEGF, IL-1 β , and TNF- α

Six WT and six COX-2 null mice underwent laser photocoagulation and were killed after 14 days. Vitreous, retina, and RPE-choroid were isolated, and a microparticle bead-based multiplex assay (Milliplex-Map kit; Millipore Corporation, Billerica, MA) was used to screen for 27 different growth factors and cytokines, including eotaxin, granulocyte colony-stimulating factor, IFN- γ , interleukin (IL)-1 α , IL-2 to IL-10, IL-12 (p40, p70), IL-13, IL-17, interferon-inducible protein, keratinocyte chemoattractant, lipopolysaccharide-induced CXC chemokine, monocyte chemoattractant protein-1, macrophage colony-stimulating factor, macrophage inflammatory protein-1a and -1b, and macrophage inflammatory protein 2. Measurable levels of VEGF, IL-1 β , and tumor necrosis factor (TNF)- α were obtained and provided the rationale for further testing.

A total of 54 (27 WT and 27 COX-2 null) mice were used to determine the expression of VEGF, IL-1 β , and TNF- α . Six WT and six COX-2 null mice were unlasered and used as controls. After laser

photocoagulation, 11 WT and 11 COX-2 null mice were killed at 24 hours, five WT and five COX-2 null mice were killed at 72 hours, and five WT and five COX-2 null mice were killed at 168 hours (7 days). Isolation of vitreous, retina, and RPE-choroid was performed. A longitudinal incision was made into the cornea, and the lens-vitreous complex was expelled. The retina was separated from the eyecup. The remaining RPE-choroid complex was then isolated. The retina and RPE-choroid were placed immediately in passive lysis buffer (Promega, Madison, WI) for 1 hour at 4°C and then frozen at -80°C for later testing. The vitreous was isolated from lens material by centrifuging for 1 minute at 20,000g using a 600 μ m filter (Sefar Nitex, Heiden, Switzerland) and immediately frozen at -80°C.

Measurement of VEGF, IL-1 β , and TNF- α

A microparticle bead-based multiplex assay was used to measure VEGF, IL-1 β , and TNF- α levels in isolated tissue samples, as previously described.^{14,15} Serial 1:4 dilutions of standards were prepared. A vacuum filtration system was used for all wash steps. Standards, control, and tissue samples were added to individual wells of a 96-well plate containing VEGF, IL-1 β , and TNF- α detection beads and incubated overnight at 4°C on an orbital shaker (300 rpm). After incubation, detection antibody was added to each well, and the plates were incubated for 30 minutes at room temperature. The plates were then washed, detection reagent (streptavidin-phycoerythrin) was added to each well, and the plates were reincubated for 10 minutes. The beads were washed, resuspended in 150 μ L wash buffer, and shaken for 30 seconds at 1100 rpm. The plates were then read by a flow cytometry-based instrument (Bio-Plex Array Reader; Bio-Rad, Hercules, CA), which uses Luminex (Austin, TX) technology. The mean fluorescence intensity for each well was determined as the mean fluorescence of 200 beads. The lower limit of detection was defined by the lowest standard, with fluorescence > background fluorescence + 2 SD of the background fluorescence. Analysis software (Bio-Plex Manager 4.1; Bio-Rad) converted fluorescence readings to concentration by use of a calibration curve derived from a five-parameter logistic fit³ of fluorescence readings of the standards. The upper limit of detection was determined by the highest standard, having measured concentration back-calculated from the standard curve within 70% of the expected value. The upper limit of detection was in all cases several orders of magnitude higher than concentrations measured in the retina, vitreous, and RPE-choroid. The quality of the fit of the standard curve to the data was good, as judged by graphical representation and the criteria that all standards between the upper and lower limits of detection had back-calculated concentrations within 70% of expected values. No concentrations were extrapolated beyond the lower or upper range of the standard curve. The final values of VEGF, IL-1 β , and TNF- α in pg/mL were normalized to total protein concentration (mg/mL) in tissue lysates to correct for differences in tissue densities, as previously described.⁶

Statistical Analysis

Results were expressed as mean \pm 95% confidence interval (CI) for image analysis and mean \pm SD for VEGF and cytokine analysis. Comparison of mean values was performed using an unpaired Student's *t*-test with unequal variance. *P* < 0.05 was considered statistically significant.

RESULTS

Fluorescein Angiography and Choroidal Mounts

Early- to mid-phase FA images at 14 days demonstrated consistent and visually detectable differences in rupture site staining and leakage between WT and COX-2 null mice (Fig. 1). COX-2 null mice had significantly less CNV leakage on FA (*P* = 0.001) with an average CNV lesion size of 3905 \pm 842 (95% CI) compared with 9264 \pm 2935 pixels for WT mice (Fig. 2).

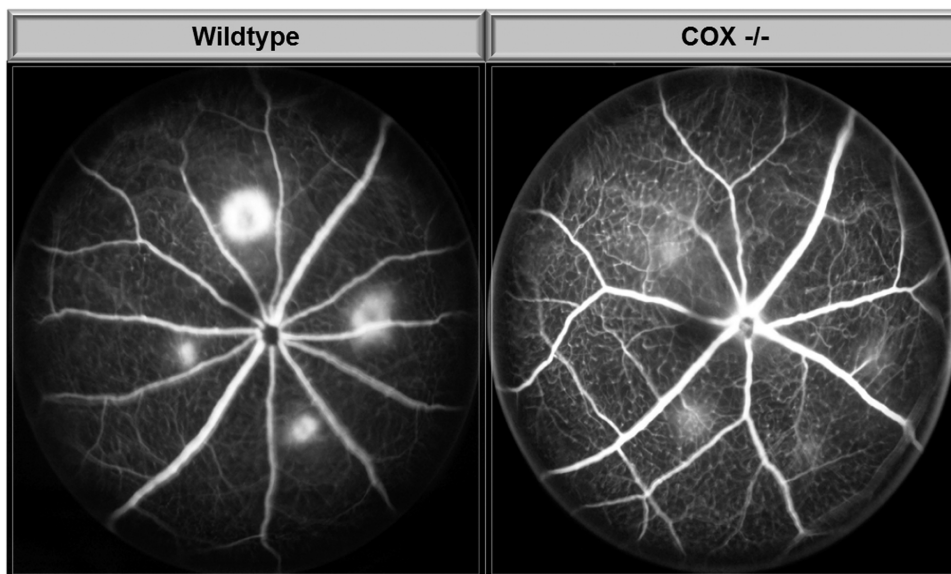


FIGURE 1. Representative fluorescein angiogram images of laser-induced CNV at 14 days.

Choroidal flat mounts at 14 days also demonstrated significant reduction in vascular budding in COX-2 null mice compared with WT (Fig. 3). COX-2 null mice demonstrated significantly ($P = 0.001$) reduced vascular budding on choroidal flat mounts, with a mean lesion size of $57,094 \pm 10,912$ pixels ($97 \pm 13 \mu\text{m}^2$ area) compared with $10,8893 \pm 27,087$ pixels ($135 \pm 16 \mu\text{m}^2$ area) for WT mice (Fig. 4).

VEGF Levels after Laser Photocoagulation

Mean VEGF concentration in the retina and RPE-choroid (combined) for unlasered WT mice was 1.2 ± 0.42 pg/mg protein. VEGF levels rose immediately after laser photocoagulation in WT mice and became significantly greater than baseline levels at 72 hours ($P < 0.01$) and 7 days ($P < 0.05$; Fig. 5). For unlasered COX-2 null mice, mean VEGF concentration was

0.42 ± 0.2 pg/mg protein, which was significantly less than unlasered WT mice ($P < 0.05$). VEGF levels rose immediately after laser photocoagulation in COX-2 null mice and became significantly greater than baseline levels at 24 hours ($P < 0.001$) but then declined slightly and were not significantly greater than baseline levels at 72 hours or 7 days. By 7 days, VEGF levels rose to 9.8 ± 6.4 pg/mg protein in WT mice versus 2.2 ± 1.7 pg/mg protein for COX-2 null mice ($P < 0.05$).

IL-1 β Levels after Laser Photocoagulation

No differences were detected in baseline IL-1 β levels in the retina and RPE-choroid of unlasered WT and COX-2 null mice ($P = 0.37$). After laser photocoagulation, IL-1 β levels rose in WT mice and were significantly greater than levels in COX-2 null mice after 72 hours (Fig. 6). Mean IL-1 β concentration at 72 hours was 10.8 ± 5.6 pg/mg protein for lasered WT mice versus 4.37 ± 0.66 pg/mg protein for lasered COX-2 null mice ($P < 0.05$). However by day 7, IL-1 β levels decline in WT mice to 4.63 ± 0.88 pg/mg protein, whereas IL-1 β levels were 8.51 ± 1.08 pg/mg protein ($P < 0.01$) in COX-2 null mice.

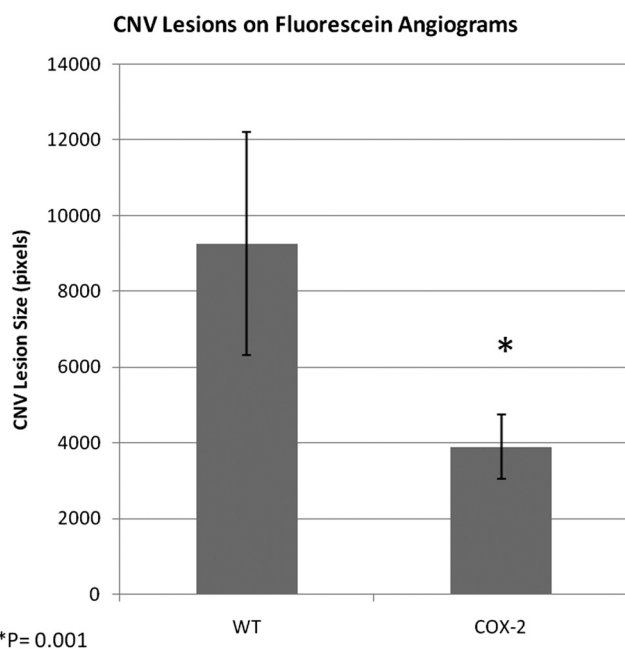
TNF- α Levels after Laser Photocoagulation

No differences were detected in baseline TNF- α levels in the retina and RPE-choroid in unlasered WT and COX-2 null mice ($P = 0.9$; Fig. 7). After laser photocoagulation, TNF- α levels were significantly greater in COX-2 null mice compared with WT mice after 72 hours ($P < 0.01$) and reached a mean concentration of 0.48 ± 0.08 pg/mg protein at day 7 versus only 0.21 ± 0.11 pg/mg protein for WT mice ($P < 0.05$).

DISCUSSION

The results of our in vivo study demonstrate that COX-2 null mice develop significantly less choroidal neovascular membrane formation than WT mice using the laser photocoagulation injury model. This finding may be explained in large part by reduced VEGF expression in COX-2 null mice, which was observed at baseline and at 7 days after laser application. To our knowledge, this is the first study to suggest a direct relationship between COX-2 and VEGF expression in choroidal neovascularization.

COX is a rate-limiting enzyme in the inflammatory process and catalyzes the biosynthesis of prostaglandins (PGD₂, PGE₂,



* $P = 0.001$

FIGURE 2. Mean pixel area of CNV lesions measured on fluorescein angiogram at 14 days after laser photocoagulation of six WT and six COX-2 mice. Error bars represent 95% CI.

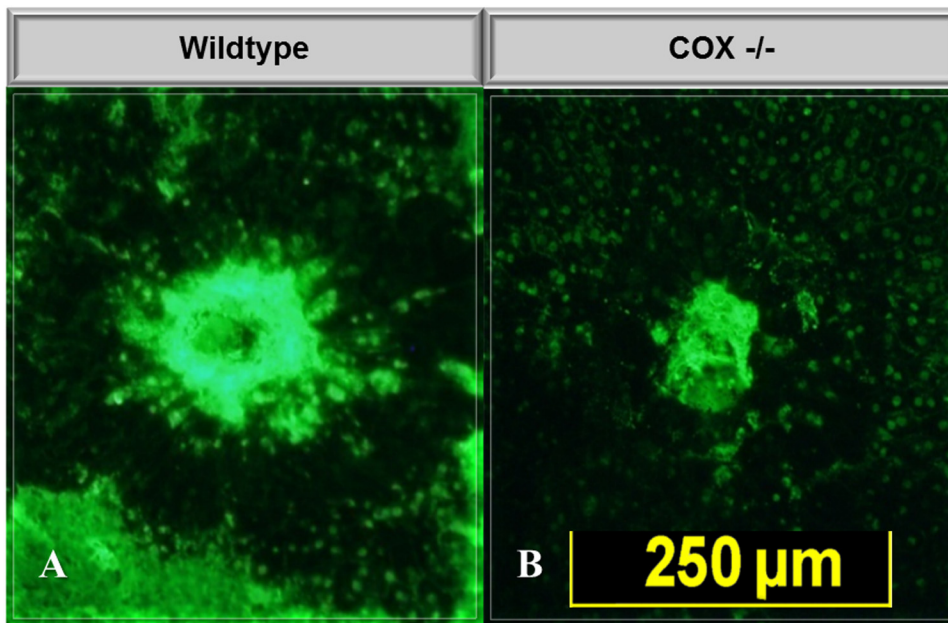


FIGURE 3. Representative choroidal flat mounts demonstrating laser-induced CNV and degree of vascular budding in WT and COX-2 null mice at 14 days. Mean CNV area was $97.2 \mu\text{m}^2$ for COX-2 null mice and $135.3 \mu\text{m}^2$ for WT mice ($P < 0.001$).

PGF_2), prostacyclin (PGI_2), and thromboxane (TXA_2). Prostaglandins have several well-established inflammatory effects within the eye, including disruption of the blood-ocular barrier and promotion of leukocyte migration.⁸ Two isoforms of COX—COX-1 and COX-2—are firmly established and are among the most thoroughly studied and best understood mammalian enzymes.¹⁶ In the human retina, COX-2 has been shown to be the predominant isoform in RPE cells and is significantly upregulated in response to proinflammatory cytokines,^{7,17} and it can be detected in human choroidal neovascular membranes.⁹

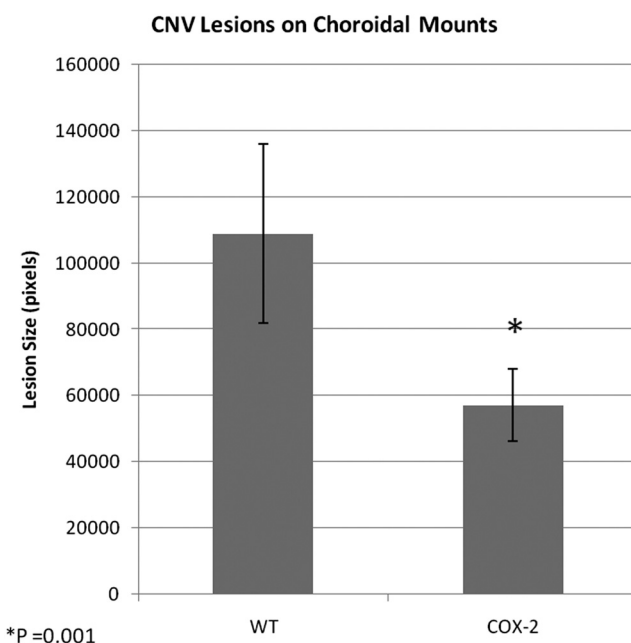
Nonsteroidal anti-inflammatory drugs (NSAIDs) are potent inhibitors of COX enzymes and, thereby, prostaglandins and are frequently used for medical therapy because of their anti-

inflammatory effects. Considerable evidence also indicates that COX-2 promotes angiogenesis.^{18,19} We and others^{4,5,10,11,20,21} have previously shown that NSAIDs inhibit CNV in animal models, and in a large retrospective study²² a reduced incidence of CNV was observed in AMD patients taking aspirin. However, though the anti-inflammatory properties of NSAIDs reside in their ability to inhibit the activity of cyclooxygenase, NSAIDs also have other biological actions, including inhibiting nuclear factor- κB , which plays a central role in the expression of various soluble proinflammatory mediators and leukocyte adhesion molecules.²³ Consequently our study provides more direct evidence for a role of COX-2 in choroidal neovascularization.

It is now firmly established that VEGF is a principal mediator of ocular angiogenesis. Previous studies have reported that COX-2 expression is increased in the retinas of diabetic animals and that COX-2 inhibition suppresses diabetes-induced upregulation of VEGF.^{24–26} Moreover, pharmacologic inhibition of COX-2 appears to reduce VEGF expression in cultured human RPE cells²⁷ and suppresses VEGF expression in both trauma-induced and ischemia-induced animal models.^{6,21,28} In vitro studies have demonstrated that PGE_2 increases VEGF expression in cultured rat Müller cells.^{6,29} In addition, agonism or antagonism of the PGE_2 receptor EP_4 increases or decreases VEGF production, respectively, in a dose-dependent manner.⁶ However, to our knowledge, this is the first study to demonstrate a direct relationship between COX-2 and VEGF expression in experimental laser-induced CNV.

Although VEGF is upregulated by several pathways, it is most consistently and robustly upregulated by hypoxia. Although retinal hypoxia from thickening of Bruch's membrane impeding oxygen exchange from the underlying choriocapillaris or reduced choroidal circulation may contribute to increased VEGF expression in AMD, there are several clinical conditions (posterior uveitis, ocular histoplasmosis) in which CNV occurs in the apparent absence of tissue hypoxia. In these conditions, local inflammation and inflammatory mediators may be the predominant pathway for VEGF expression.³⁰

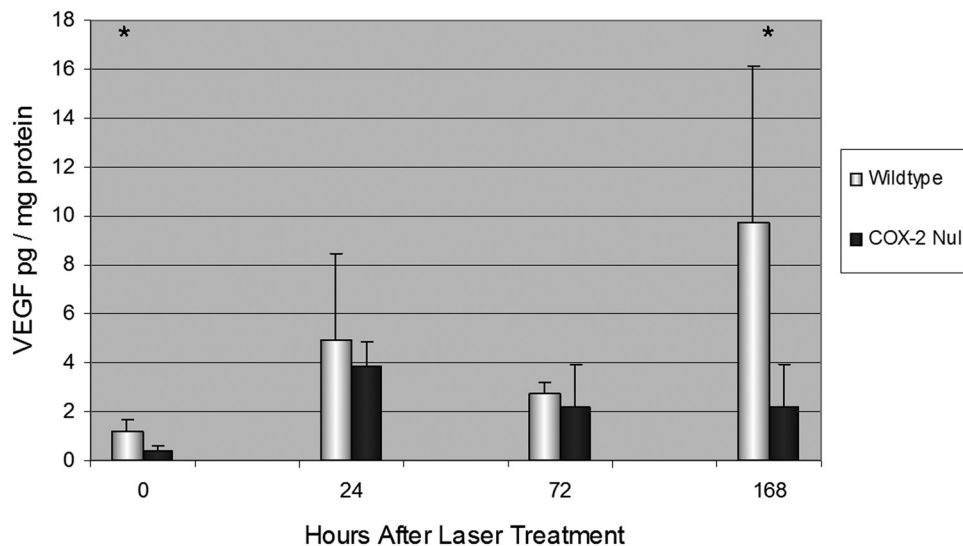
Consequently, laser-induced CNV is an appropriate model with which to investigate the relationship between inflammation and VEGF expression. Histologic studies demonstrate the immediate arrival of macrophages at laser rupture sites within



* $P = 0.001$

FIGURE 4. Mean pixel area of CNV lesions measured on choroidal flat mounts at 14 days after laser photocoagulation of six WT and six COX-2 mice. Error bars represent 95% CI.

FIGURE 5. Mean VEGF concentration in the retina and RPE-choroid in unlasered mice (time 0) and at 24, 72, and 168 hours after laser-induced CNV. VEGF concentration was significantly greater in WT than in COX-2 null mice at time 0 and at 168 hours. Error bars are in SD. Total numbers of mice per group were as follows: time 0, 6 WT and 6 COX-2; time 24, 11 WT and 11 COX-2; time 72, 5 WT and 5 COX-2; time 168, 5 WT and 5 COX-2. * $P < 0.05$.



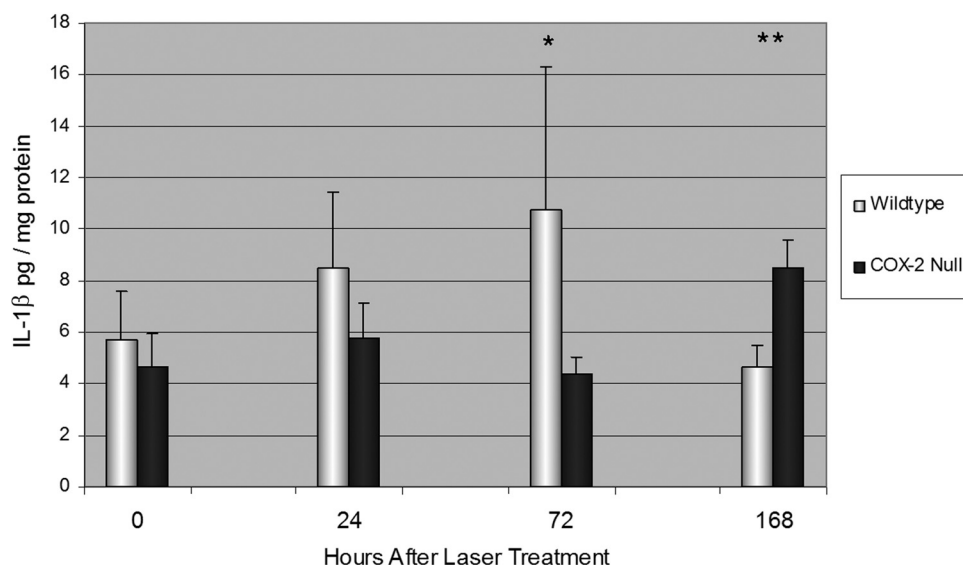
1 hour of laser application,³¹ and macrophages accumulate in areas of disruption of Bruch's membrane.^{32,33} Macrophages secrete IL-1 β , among other inflammatory cytokines, in response to tissue injury, and exposure of cultured human RPE cells to IL-1 β increases PGE₂ production by 250-fold.⁷ Our results demonstrate that IL-1 β levels rise immediately in the retina and choroid in the setting of laser photocoagulation, and we have previously demonstrated a similarly rapid increase in PGE₂.²⁰

Taken together, the following sequence of events may occur after laser photocoagulation: within the first hour of laser rupture of Bruch's membrane, there is immediate recruitment of macrophages, which secrete IL-1 β in response to tissue injury.³¹ IL-1 β upregulates COX-2 expression in neighboring RPE cells, increasing local production of PGE₂.⁷ By both autocrine and paracrine pathways, PGE₂ increases VEGF expression in the RPE and other resident retinal cells.^{6,29} PGE₂ would also amplify macrophage recruitment by disrupting the blood-ocular barrier and assisting migration.⁸ In conjunction with increased retinal VEGF, compromise of the physical barrier of Bruch's membrane³⁴ promotes choroidal angiogenesis.

According to this pathway, the absence of COX-2 or its pharmacologic inhibition would reduce VEGF expression and

account for the inhibitory effect observed with NSAIDs on CNV. Although COX-2 is the isoform thought to be predominantly upregulated in the RPE, we also observed upregulation of COX-1 in cultured RPE cells exposed to cytokines (data not shown), which might have contributed to the choroidal neovascular membrane formation observed in our COX-2 null mice after laser application. Our observation that COX-2 null mice have a delayed rise in IL-1 β levels compared with the more rapid rise (and then fall) of IL-1 β levels in WT mice can be plausibly explained by reduced retinal prostaglandins, which normally increase immediately after laser photocoagulation²⁰ and promote blood vessel permeability and recruitment of inflammatory cells (source of IL-1 β). Increased production of TNF- α in COX-2 null mice compared with WT mice may also be the result of decreased prostaglandins. Shinomiya et al.³⁵ have previously reported that PGE₂ directly (by way of its receptors EP₂ and EP₄) downregulates TNF- α production in murine macrophages stimulated with zymosan, which can be reversed by the NSAID indomethacin. Their work³⁵ suggests that endogenous prostaglandins have a regulatory effect on TNF- α production and is consistent with our observation of increased TNF- α in COX-2 null (prostaglandin depleted) mice after laser photocoagulation.

FIGURE 6. Mean IL-1 β concentration in the retina and RPE-choroid in unlasered mice (time 0) and at 24, 72, and 108 hours after LCNV. IL-1 β concentration was greater in WT than in COX-2 null mice at 24 ($P = 0.15$) and 72 hours ($P < 0.05$) but became significantly less at 168 hours ($P < 0.01$). Error bars are in SD. Total numbers of mice per group were as follows: time 0, 6 WT and 6 COX-2; time 24, 11 WT and 11 COX-2; time 72, 5 WT and 5 COX-2; and time 168, 5 WT and 5 COX-2. * $P < 0.05$. ** $P < 0.01$.



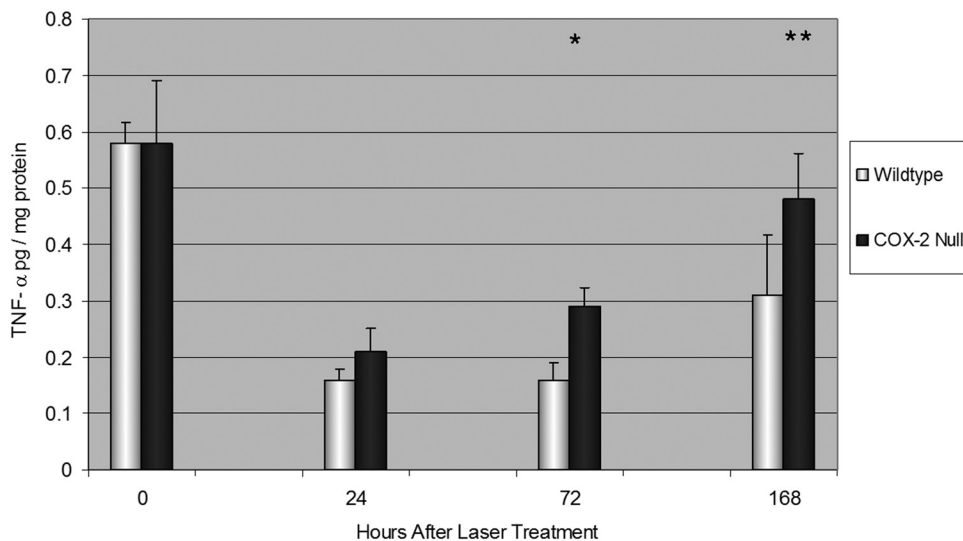


FIGURE 7. Mean TNF- α concentration in the retina and RPE-choroid in unlasered mice (time 0) and at 24, 72, and 168 hours after LCNV. TNF- α concentration was significantly greater in COX-2 null than in WT mice at 72 ($P < 0.01$) and 168 hours ($P < 0.05$). Error bars are in SD. Total numbers of mice per group were as follows: time 0, 6 WT and 6 COX-2; time 24, 11 WT and 11 COX-2; time 72, 5 WT and 5 COX-2; time 168, 5 WT and 5 COX-2. * $P < 0.01$. ** $P < 0.05$.

In conclusion, COX-2 null mice exhibited significantly less choroidal neovascular membrane formation, possibly because of reduced expression of VEGF. The results of this study suggest that COX-2 modulates VEGF expression in laser-induced choroidal neovascularization and suggest a potential therapeutic role for NSAIDs.

References

- Kedhar SR, Thorne JE, Wittenberg S, Dunn JP, Jabs DA. Multifocal choroiditis with panuveitis and punctate inner choroidopathy: comparison of clinical characteristics at presentation. *Retina*. 2007;27:1174-1179.
- Soubrane G. Choroidal neovascularization in pathologic myopia: recent developments in diagnosis and treatment. *Surv Ophthalmol*. 2008;53:121-138.
- Cohen SY, Laroche A, Leguen Y, Soubrane G, Coscas GJ. Etiology of choroidal neovascularization in young patients. *Ophthalmology*. 1996;103:1241-1244.
- Kim SJ, Toma HS. Inhibition of choroidal neovascularization by intravitreal ketorolac. *Arch Ophthalmol*. 2010;128:596-600.
- Takahashi H, Yanagi Y, Tamaki Y, Uchida S, Muranaka K. COX-2-selective inhibitor, etodolac, suppresses choroidal neovascularization in a mice model. *Biochem Biophys Res Commun*. 2004;325:461-466.
- Yanni SE, Barnett JM, Clark ML, Penn JS. The role of PGE2 receptor EP4 in pathologic ocular angiogenesis. *Invest Ophthalmol Vis Sci*. 2009;50:5479-5486.
- Chin MS, Nagineni CN, Hooper LC, Detrick B, Hooks JJ. Cyclooxygenase-2 gene expression and regulation in human retinal pigment epithelial cells. *Invest Ophthalmol Vis Sci*. 2001;42:2338-2346.
- Kim SJ, Flach AJ, Jampol LM. Nonsteroidal anti-inflammatory drugs in ophthalmology. *Surv Ophthalmol*. 2010;55:108-133.
- Maloney SC, Fernandes BF, Castiglione E, et al. Expression of cyclooxygenase-2 in choroidal neovascular membranes from age-related macular degeneration patients. *Retina*. 2009;29:176-180.
- Hu W, Criswell MH, Ottleczyk A, et al. Oral administration of lumiracoxib reduces choroidal neovascular membrane development in the rat laser-trauma model. *Retina*. 2005;25:1054-1064.
- Sakamoto T, Soriana D, Nassaralla J, et al. Effect of intravitreal administration of indomethacin on experimental subretinal neovascularization in the subhuman primate. *Arch Ophthalmol*. 1995;113:222-226.
- Edelman JL, Castro MR. Quantitative image analysis of laser-induced choroidal neovascularization in rat. *Exp Eye Res*. 2000;71:523-533.
- Toma HS, Barnett JM, Penn JS, Kim SJ. Improved assessment of laser-induced choroidal neovascularization. *Microvasc Res*. 2010;80:295-302.
- Vignali DA. Multiplexed particle-based flow cytometric assays. *J Immunol Methods*. 2000;243:243-255.
- Carson RT, Vignali DA. Simultaneous quantitation of 15 cytokines using a multiplexed flow cytometric assay. *J Immunol Methods*. 1999;227:41-52.
- Rouzer CA, Marnett LJ. Cyclooxygenases: structural and functional insights. *J Lipid Res*. 2009;50:S29-S34.
- Vane JR, Bakhle YS, Botting RM. Cyclooxygenases 1 and 2. *Annu Rev Pharmacol Toxicol*. 1998;38:97-120.
- Monnier Y, Zaric J, Ruegg C. Inhibition of angiogenesis by non-steroidal anti-inflammatory drugs: from the bench to the bedside and back. *Curr Drug Targets Inflamm Allergy*. 2005;4:31-38.
- Gately S, Kerbel R. Therapeutic potential of selective cyclooxygenase-2 inhibitors in the management of tumor angiogenesis. *Prog Exp Tumor Res*. 2003;37:179-192.
- Kim SJ, Toma HS, Barnett JM, Penn JS. Ketorolac inhibits choroidal neovascularization by suppression of retinal VEGF. *Exp Eye Res*. 2010;91:537-543.
- Takahashi K, Saishin Y, Saishin Y, et al. Topical nepafenac inhibits ocular neovascularization. *Invest Ophthalmol Vis Sci*. 2003;44:409-415.
- Wilson HL, Schwartz DM, Bhatt HR, et al. Statin and aspirin therapy are associated with decreased rates of choroidal neovascularization among patients with age-related macular degeneration. *Am J Ophthalmol*. 2004;137:615-624.
- Ghosh S, May MJ, Kopp EB. NF-kappa B and Rel proteins: evolutionarily conserved mediators of immune responses. *Annu Rev Immunol*. 1998;16:225-260.
- Ayalasomayajula SP, Amrite AC, Kompella UB. Inhibition of cyclooxygenase-2, but not cyclooxygenase-1, reduces prostaglandin E2 secretion from diabetic rat retinas. *Eur J Pharmacol*. 2004;498:275-278.
- Kern TS. Contributions of inflammatory processes to the development of the early stages of diabetic retinopathy. *Exp Diabetes Res*. 2007;2007:95-103.
- Ayalasomayajula SP, Kompella UB. Celecoxib, a selective cyclooxygenase-2 inhibitor, inhibits retinal vascular endothelial growth factor expression and vascular leakage in a streptozotocin-induced diabetic rat model. *Eur J Pharmacol*. 2003;458:283-289.
- Amrite AC, Ayalasomayajula SP, Cheruvu NP, Kompella UB. Single periocular injection of celecoxib-PLGA microparticles inhibits diabetes-induced elevations in retinal PGE2, VEGF, and vascular leakage. *Invest Ophthalmol Vis Sci*. 2006;47:1149-1160.
- Yanni SE, McCollum GW, Penn JS. Genetic deletion of COX-2 diminishes VEGF production in mouse retina Muller cells. *Exp Eye Res*. 2010;91:34-41.
- Cheng T, Cao W, Wen R, Stenberg RH, LaVail MM. Prostaglandin E2 induces vascular endothelial growth factor and basic fibroblast growth factor mRNA expression in cultured rat Muller cells. *Invest Ophthalmol Vis Sci*. 1998;39:581-591.
- Lee SH, Kim MH, Han HJ. Arachidonic acid potentiates hypoxia-induced VEGF expression in mouse embryonic stem cells: involve-

- ment of Notch, Wnt, and HIF-1 α . *Am J Physiol Cell Physiol*. 2009;297:C207–C216.
31. Miller H, Miller B, Ishibashi T, Ryan SJ. Pathogenesis of laser-induced choroidal subretinal neovascularization. *Invest Ophthalmol Vis Sci*. 1990;31:899–908.
 32. Grossniklaus HE, Ling JX, Wallace TM, et al. Macrophage and retinal pigment epithelium expression of angiogenic cytokines in choroidal neovascularization. *Mol Vis*. 2002;8:119–126.
 33. Lopez PF, Grossniklaus HE, Lambert HM, et al. Pathologic features of surgically excised subretinal neovascular membranes in age-related macular degeneration. *Am J Ophthalmol*. 1991;112:647–656.
 34. Yu HG, Liu X, Kiss S, et al. Increased choroidal neovascularization following laser induction in mice lacking lysyl oxidase-like 1. *Invest Ophthalmol Vis Sci*. 2008;49:2599–2605.
 35. Shinomiya S, Naraba H, Ueno A, et al. Regulation of TNF α and interleukin-10 production by prostaglandins I(2) and E(2): studies with prostaglandin receptor-deficient mice and prostaglandin E-receptor subtype-selective synthetic agonists. *Biochem Pharmacol*. 2001;61:1153–1160.